Development and Characterization of a Novolac Resin/$BaTiO_3$ Nanoparticles Composite System

I. Asimakopoulos,[1,2] L. Zoumpoulakis,[2] G. C. Psarras[1]

[1]*Department of Materials Science, School of Natural Sciences, University of Patras, Patras 26504, Greece*
[2]*National Technical University of Athens, School of Chemical Engineering, Section III "Materials Science and Engineering", Laboratory Unit "Advanced and Composite Materials", Zografou Campus, Athens 157 73, Greece*

Received 14 March 2011; accepted 21 November 2011
DOI 10.1002/app.36518
Published online in Wiley Online Library (wileyonlinelibrary.com).

ABSTRACT: Polymer composites incorporating ferroelectric and piezoelectric crystal particles, randomly distributed within the host matrix, represent a novel class of materials. In this study, composite materials consisted of novolac resin and barium titanate nanoparticles were prepared and examined, varying the nanofiller content. Structural characterization was conducted via X-ray diffraction and scanning electron microscopy. Mechanical and dielectric properties were examined by employing bending and shear strength tests and broadband dielectric spectroscopy, respectively. Bending and shear strength found to decrease with the filler content. Dielectric permittivity was found to increase significantly with filler content, and the detected relaxation processes were attributed to interfacial polarization, glass to rubber transition of the matrix, and reorientation of polar side groups of the polymer chain. Although, the mechanical performance of the examined systems seems not to be attractive in applications due to its brittleness, nanocomposites' dielectric response could be proved interesting in electrical and electronic devices applications.
 J Appl Polym Sci 000: 000–000, 2012

Key words: polymer nanocomposites; novolac; ferroelectric crystal; barium titanate; mechanical properties; broadband dielectric spectroscopy

INTRODUCTION

In our days, the increasing demands and the competing characteristics on the performance of materials and structures require the development of new classes of materials with advanced properties or behavior. Functional or smart materials are materials systems able to control some of their physical characteristics like the natural vibrational frequency, the coefficient of damping capacity, their shape, their polarization etc., in response to an appropriate stimulus.[1,2] Recently ceramic–polymer composites have been studied in various applications including integrated capacitors, acoustic emission sensors, and for the reduction of leakage currents.[3–5] Furthermore, if the embedded ceramic particles are ferroelectric, functional, or self-tunable properties can be disclosed to the composite structure. Ferroelectric materials exhibit spontaneous polarization and are characterized by a temperature-dependent disorder to order transition. The electrical response of polymer matrix particulate composites depends on various factors such as the permittivity and conductivity of the constituent phases, the size, shape and volume fraction of the filler, and the type of distribution of additives.

Correspondence to: G. C. Psarras (G.C.Psarras@upatras.gr).

Composite materials of this type are not well-known for their remarkable mechanical properties, but for their specialized electrical response. Ceramic–polymer composites consisting of piezo/ferroelectric crystal particles (such as $BaTiO_3$), homogeneously distributed, in the polymer host represent a novel class of materials, which exhibit several interesting properties.[6–11] High-tech electronic devices require new high dielectric permittivity materials (known as high-K materials), which combine, at the same time, suitable dielectric properties, tunable polarization, energy storing efficiency, and easy processing.[12–15]

In this study, novel composite systems have been produced, by integrating ceramic barium titanate nanoparticles within a phenolic (novolac) resin, at various filler loadings. Produced systems were tested by means of different experimental techniques in order to assess their morphology, mechanical and dielectric properties, and functional response. X-ray diffraction, scanning electron microscopy, mechanical tests, and broadband dielectric spectroscopy scans provided the aforementioned information.

EXPERIMENTAL

Samples preparation

Composite specimens were prepared by employing commercially available materials. Barium titanate

was purchased by Sigma-Aldrich. The mean particle diameter was less than 50 nm. Novolac resin is a phenol-formaldehyde resin and was created in our laboratory by progressive polymerization. The synthesis of novolac resin, comprises the polycondensation of phenol (Merck) with the presence of formaldehyde (Fluka), as catalyst has been used acetic acid (Fluka).[16,17] Hexamethylenotetramine, purchased by Merck, was used as the curing agent. The preparation procedure involved the following steps: At the first stage, novolac and hardener (hexa) were pulverized. After being carefully selected from a sieve that allows only particles smaller than 300 μm to pass from novolac and hexa, the pre-selected amounts of $BaTiO_3$ were added (0% w/w, 3% w/w, 5% w/w, 10% w/w, 15% w/w, 20% w/w $BaTiO_3$). The novolac powder was mixed with Hexa powder in the ratio of 7:2 w/w, the specific amount of barium titanate powder was consequently added and all of them were mixed in order to produce a macroscopically homogenous powder.

After homogenization samples were cured and postcured in the thermo-compressor. The curing process lasted for 1 h at 140°C, and the postcuring process lasted for another hour at 170°C while applying pressure of 8.5 MPa.[18,19]

Morphological characterization

X-ray diffraction (XRD) (Siemens D5000, using a Cu Ka source, scanning in the range 5 to 120°, with a step of 0.0020° and a step time of 1 s) characterization was carried out on the following samples: 0% (pure and cured novolac), composites with 3% w/w, 10% w/w, and 20% w/w $BaTiO_3$ and pure $BaTiO_3$ powder. Furthermore, specimens' morphology was examined by means of scanning electron microscopy (FEI Quanta 200 Scanning Electron Microscope) equipped with element dispersive X-ray analysis (EDAX). Filler distribution within the specimens is characterized as satisfactory, and as expected both clusters and nanodispersions coexist, Figure 2. The insulating nature of this type of composite materials acts as a restriction, upon the resolution of SEM imaging. Nevertheless, because of the backscattered electrons satisfactory images can be taken. Images reveal voids, created during curing process, clusters, and isolated barium titanate particles. Image contrast distinguish barium titanate particles from the polymer matrix, since they appear as "white rocks," while polymer matrix appears as "dark sea". EDAX measurements (Table I), verify the presence of barium titanate, while polymer matrix contributes in the detected carbon percentage.

TABLE I
Values of EDAX Measurements for the Sample with 5% w/w $BaTiO_3$ Content

Element	C	O	Ba(L)	Ti(K)	Total
Percentage %	66.62	2.75	25.15	5.49	100.00

Mechanical characterization

Composite specimens were mechanically tested using the three-point method, employing bending (DIN-53452) and shear (ASTM-NORM D 2344-65T) strength tests.[20] The only difference between these two tests is the following: in the shear strength test the distance between the two points was 10 mm, while in the bending strength test was 100 mm. In both of them, the evaluated parameter was the deflection in μm. The whole experiment took place at room temperature, 25°C. Specimens' dimensions were 17 mm width, 3 mm thickness, and more than 10 mm length for shear tests, while specimens' dimensions, for bending tests, were 1 mm width, 3 mm thickness, and more than 100 mm length. Values of shear and bending deflection, as well as the corresponding strength values[20,21] are listed in Table II.

Dielectric measurements

Dielectric measurements were conducted by means of broadband dielectric spectroscopy (BDS) in the frequency range of 0.1 Hz to 10 MHz, using an Alpha-N Frequency Response Analyser (Novocontrol Technologies, Hundsagen, Germany). The employed dielectric cell (BDS-1200, Novocontrol) is a parallel-plate capacitor with two gold-plated electrodes. Temperature was controlled via Novotherm device, supplied also by Novocontrol. Experimental

TABLE II
Values of Shear, Bending Deflection, and Shear, Bending Strength for All the Examined Systems

Sample	Shear's deflection (μm)	Bending's deflection (μm)	Shear strength (MPa)	Bending strength (MPa)
Resin+0% w/w $BaTiO_3$	7.5	1.00	1.81	24.44
Resin+3% w/w $BaTiO_3$	6.1	0.20	1.47	4.89
Resin+5% w/w $BaTiO_3$	2.8	0.15	0.68	3.67
Resin+10% w/w $BaTiO_3$	1.8	0.10	0.43	2.44
Resin+15% w/w $BaTiO_3$	1.8	0.05	0.43	1.22
Resin+20% w/w $BaTiO_3$	1.4	0.02	0.34	0.49

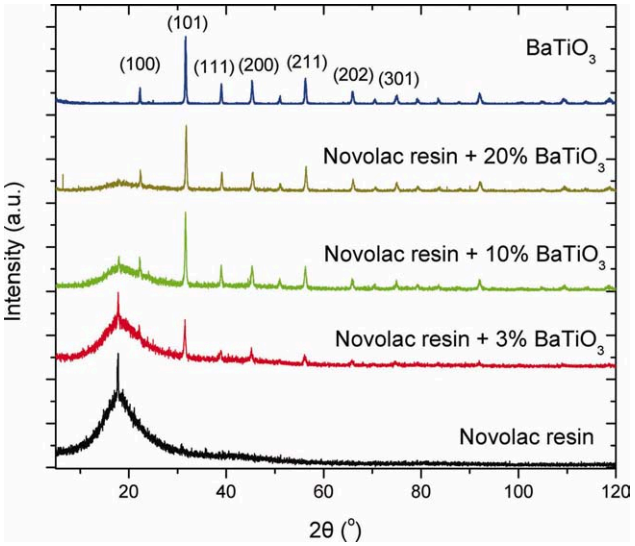

Figure 1 XRD spectra of the systems with 0, 3, 10, 20, and 100% w/w content in $BaTiO_3$ nanoparticles (bottom to up). [Color figure can be viewed in the online issue, which is available at wileyonlinelibrary.com.]

data were obtained by performing isothermal frequency scans, for each examined specimen, from ambient to 150°C with a temperature step of 5°C. The amplitude of the applied test voltage was kept constant at 1000 mV.

RESULTS AND DISCUSSION

The XRD spectra of pure novolac resin, all composite systems, and $BaTiO_3$ powder are depicted in Figure 1. The crystalline nature of $BaTiO_3$ is reflected in its spectrum, via the formation of sharp peaks, noted on the graph. The presence of barium titanate particles in all composites becomes evident via the formation of the characteristic peaks, the intensity of which increase with the $BaTiO_3$ content. Pure novolac displays a broad peak in its spectrum, the intensity of which diminishes, in the case of the nanocomposites, with the percentage of barium titanate. Consequently, the XRD spectra can be employed, not only for the qualitative verification of the composite systems composition, but after a normalization procedure for the estimation of the corresponding proportions of each component in similar composite materials. Figure 2 provides typical SEM images of the examined nanosystems. Ceramic nanofiller appear to be satisfactory distributed, while images reveal the presence of both nanodispersions and clusters. At the two higher barium titanate contents (not shown here) extensive voids can be detected between matrix and filler. Thus, the dielectric response of these composites, although presented here, it is not considered as reliable.

Figure 3 depicts shear and bending strength (MPa) versus deflection (μm) for all the examined specimens. Table II summarizes shear-bending deflection and shear-bending strength values for all the examined systems.

From Figure 3, it results that the bending strength is decreased, as long as the percentage of barium titanate is increased. Thus the 20% w/w in barium titanate composite sample presents the minimal strength in bending. Still we observe a huge strength's reduction of the 3% w/w in barium titanate sample in comparison with the 0% w/w in barium titanate sample (pure novolac). Therefore, it can be concluded that because of the presence of barium titanate, an important reduction of strength values take place. Further, it should be noted that the ultimate failure of all samples had the characteristics of a fragile fracture. Consequently, phenomena such as necking did not appear. On the contrary, the fracture was abrupt and instantaneous. As far as shear strength of the composites is concerned, once again it can be observed a declining tendency of shear

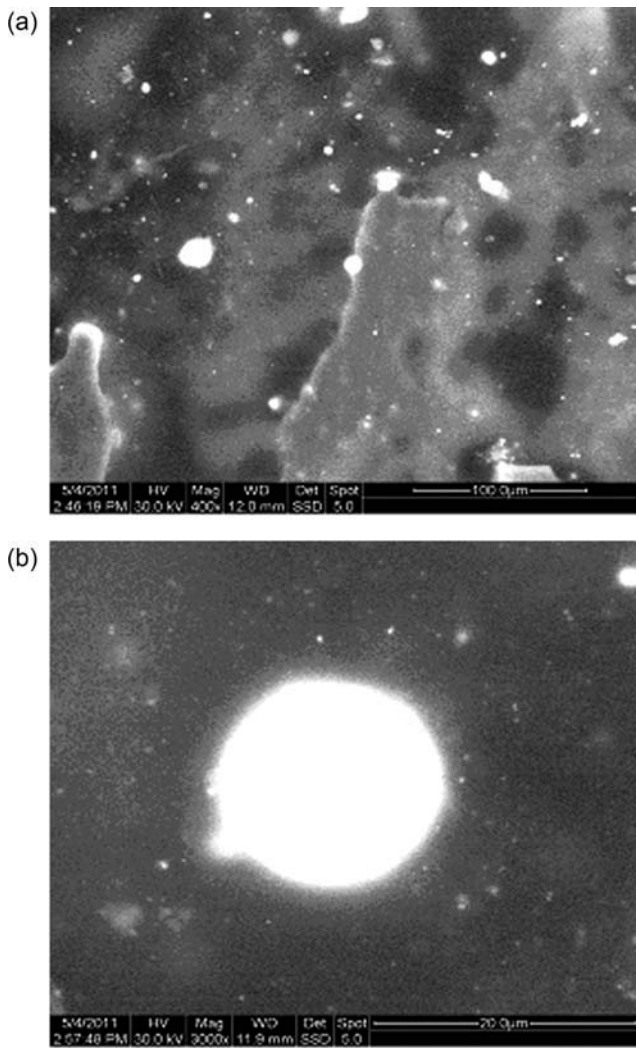

Figure 2 SEM images from the composite specimen with 5% w/w $BaTiO_3$ content at two different magnifications.

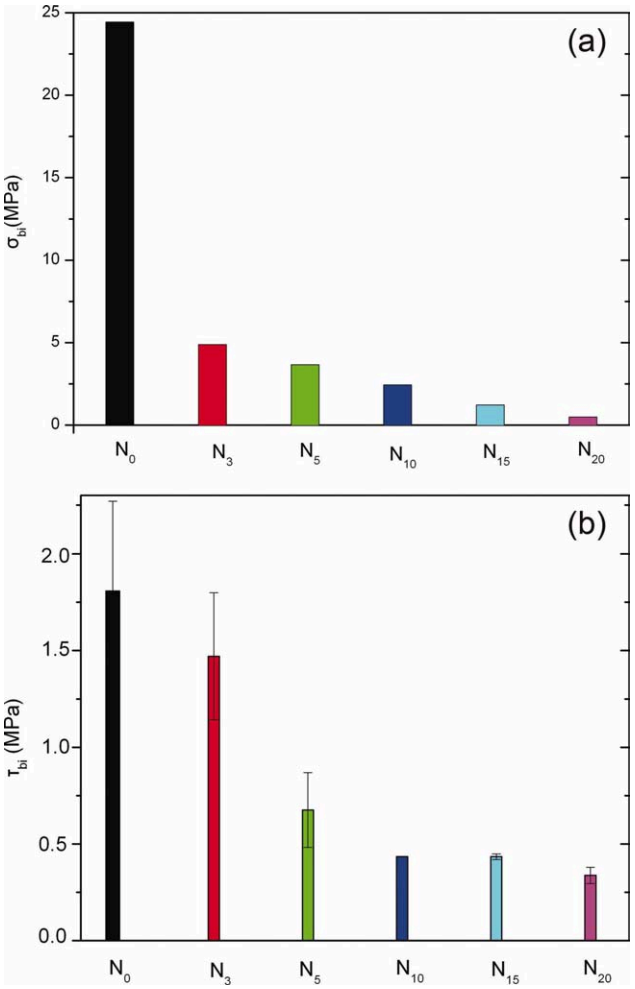

Figure 3 Bending (a) and shear (b) strength for each sample. Subscripts denote the w/w percentage of barium titanate in each sample. [Color figure can be viewed in the online issue, which is available at wileyonlinelibrary.com.]

strength with increasing the barium titanate content. A notable difference with respect to the bending strength is that now the shear strength, does not present as huge reduction of its values with ceramic filler, as it happens in the respective bending plot. Although, a lower rate of strength reduction takes place in shear mode, the ultimate failure is again abrupt and instantaneous implying a fragile fracture.

In polymer composite systems dielectric relaxation effects arise from the polymer matrix (α, β and γ-relaxation), interfacial phenomena, and conductivity effects. In many cases, at low frequencies and high temperatures space charges build up at the interface between specimen and electrodes giving rise to the parasitic phenomenon of electrode polarization, which leads to enormous values of the real and imaginary part of dielectric permittivity.[22,23] In this study the obtained dielectric data were first expressed in terms of real and imaginary part of dielectric permittivity and then transformed via eq. (1) to the electric modulus presentation. Electrical relaxation phenomena present in composite systems can be described via different formalisms, such as dielectric permittivity, electric modulus, ac conductivity, and tanδ. However, a specific formalism could be proved more effective, under some circumstances, in extracting information concerning the occurring physical mechanisms. Electric modulus presentation has been proved suitable for neglecting the influence of electrode polarization upon dielectric data; arguments have been exhibited and discussed elsewhere[22–24] Electric modulus is defined as the inverse quantity of complex permittivity, as shown in eq. (1):

$$M^* = \frac{1}{\varepsilon^*} = \frac{1}{\varepsilon' - j\varepsilon''} = \frac{\varepsilon'}{\varepsilon'^2 + \varepsilon''^2} + j\frac{\varepsilon''}{\varepsilon'^2 + \varepsilon''^2} = M' + jM'' \tag{1}$$

where ε′, M' and ε″, M'' are the real and the imaginary parts of dielectric permittivity and electric modulus, respectively.

Figure 4 depicts the variation of the real part of permittivity with the frequency of the applied field at 30°C, for all the examined systems. In all cases permittivity diminishes with frequency, reflecting the reduction of the achieved polarization. As the frequency increases permanent and induced dipoles fail to follow the alternation of the applied filed. Between 1 and 10 Hz permittivity becomes, practically, independent from frequency. Increase of filler content leads to a systematic increase of (ε′) since permittivity values of barium titanate are remarkable higher than the corresponding of novolac resin. Systems with the two higher concentrations of $BaTiO_3$ decline from this tendency exhibiting lower values

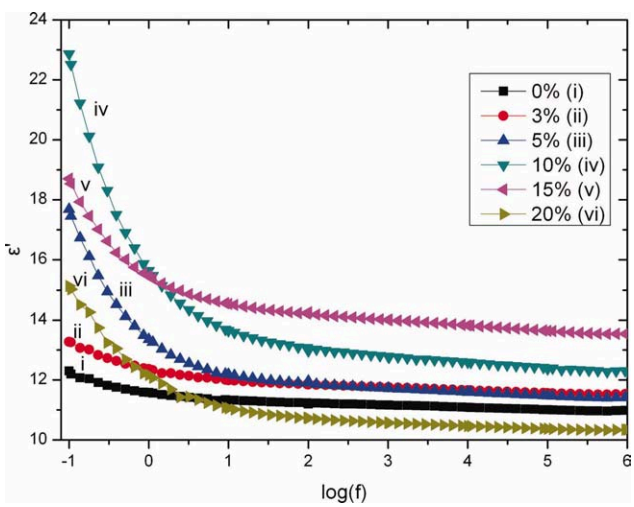

Figure 4 Real part of dielectric permittivity as a function of frequency, for all the examined systems, at 30°C. The indicated percentages represent the w/w content in $BaTiO_3$. [Color figure can be viewed in the online issue, which is available at wileyonlinelibrary.com.]

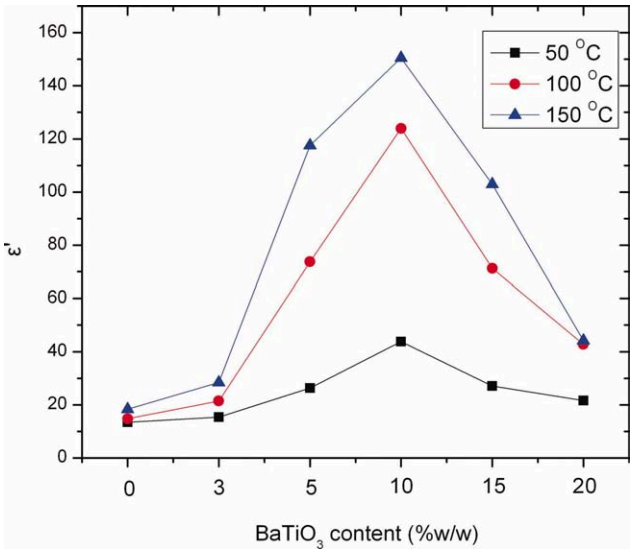

Figure 5 Real part of dielectric permittivity as a function of barium titanate percentage content at 0.1 Hz, for three different temperatures (50, 100, and 150°C). Lines are eye guides. [Color figure can be viewed in the online issue, which is available at wileyonlinelibrary.com.]

of (ε′). The occurred discrepancy is attributed to the quality of the produced samples, since at the two higher concentrations of $BaTiO_3$ nanoparticles, mixing with the polymer matrix was difficult, resulting in a nonhomogeneous distribution of ceramic particles. The specific two specimens suffered from voids and clusters. Phenolic matrix-based composites exhibit porosity because of their curing mechanism, which is a step-polymerization process and especially polycondensation in opposite to the curing mechanism of other resins.[25]

The dielectric reinforcing efficiency of barium titanate nanoparticles is clearly depicted in Figure 5, where the real part of dielectric permittivity is presented as a function of barium titanate content, at 0.1 Hz and for three different temperatures (50, 100, and 150°C). It is obvious from the diagram that dielectric permittivity increases with both barium titanate content and temperature. Under isothermal conditions (ε′) raises steeply with filler content up to the specimen with 10% w/w $BaTiO_3$ concentration, indicating the enhancement of energy storing capability of the systems. Specimens with higher concentrations of $BaTiO_3$ nanoparticles, namely 15% w/w and 20% w/w, deviate from this general tendency, because of their increased porosity and the entrapped air inside of them. Temperature acts as an accelerating parameter upon the reinforcing efficiency of barium titanate nanoparticles, since values of (ε′) grow up by a factor of 2 at 50°C compared with the values of pure matrix. The raising factor, in the case of 150°C, exceeds the value of 8. Figure 5 signifies that the optimum dielectric reinforcement is achieved at the 10%w/w barium titanate content. The remarkable increase of the real part of dielectric permittivity with temperature at this filler content, besides the presence of $BaTiO_3$, is related to the enhanced interfacial polarization due to the increased heterogeneity of the system.

The energy per volume or density of energy is proportional to the real part of dielectric permittivity and the square of the electric field intensity. Figure 6(a) displays isothermal plots of the density of energy for all the examined systems up to 10% w/w in $BaTiO_3$ content. It is evident that the energy storing efficiency steeply increases with filler content, in the whole frequency range. On the other hand, Figure 6(b) presents isochronal plots normalized upon the pure resin efficiency. The 10% w/w $BaTiO_3$ reinforced system exhibits an energy reinforcing efficiency increased by a factor of almost 8, at

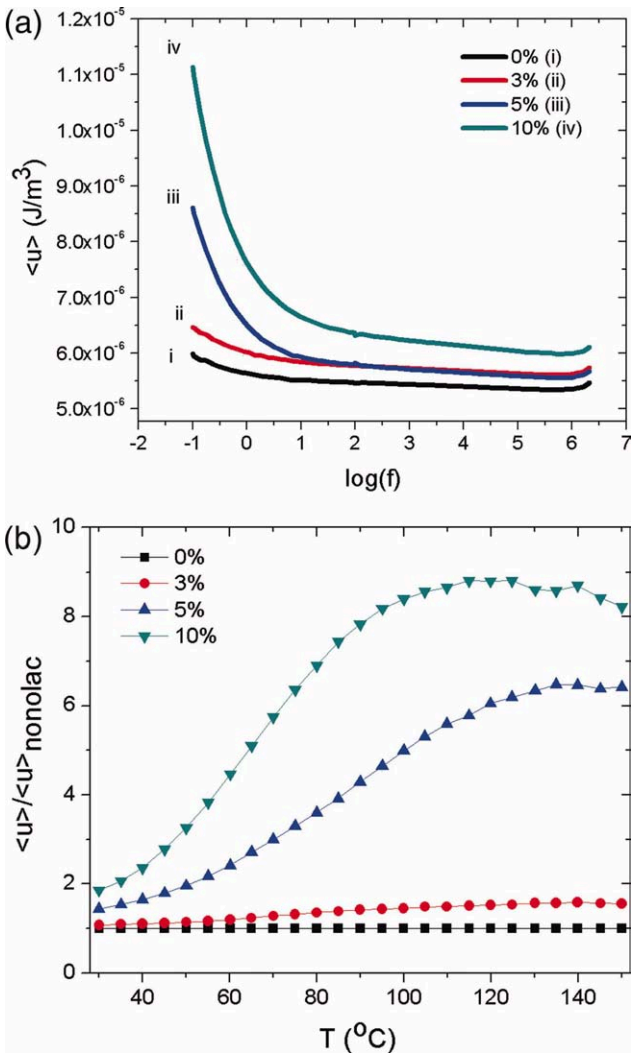

Figure 6 (a) Density of energy as a function of frequency at 30°C and (b) normalized density of energy upon the pure novolac specimen as a function of temperature at 0.1 Hz, for the examined systems. [Color figure can be viewed in the online issue, which is available at wileyonlinelibrary.com.]

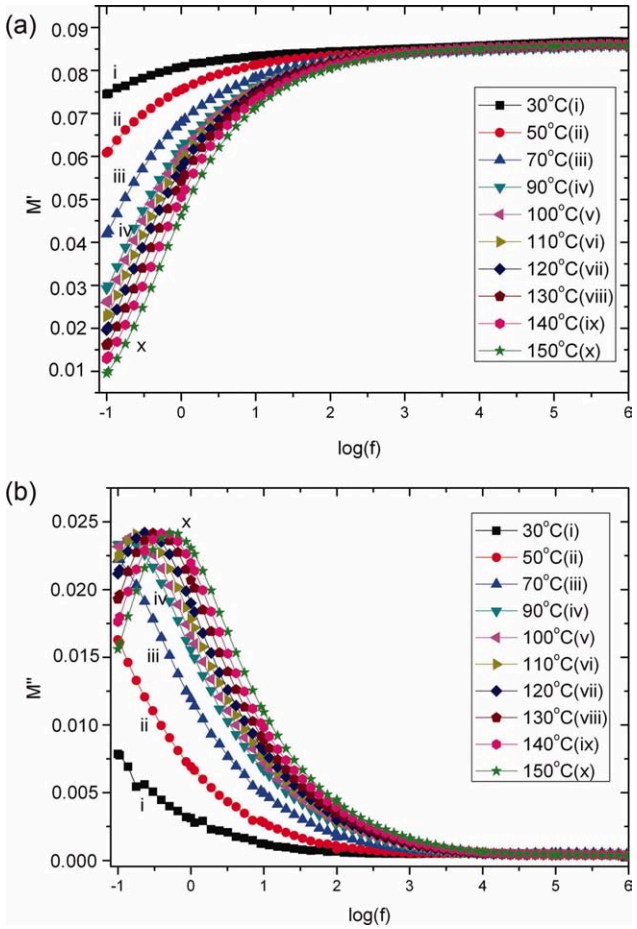

Figure 7 Real (a) and imaginary (b) part of electric modulus versus frequency for the specimen with 3% w/w content in $BaTiO_3$, at various temperatures. [Color figure can be viewed in the online issue, which is available at wileyonlinelibrary.com.]

temperature above 90°C, with respect to the pure novolac system. However, it should be noted that the energy storing efficiency is both altered and limited by the applied field's intensity. The energy per volume enhances with the field, but at a value of the applied field dielectric breakdown occurs. This value acts as a restricting factor for the service life of the specimen and also sets a limit to the energy storing efficiency. In this study electric field kept at low level, varying slightly with the specimens' thickness. The effect of strong fields and the determination of the systems' dielectric breakdown strength were not experimentally feasible to be investigated.

Figures 7 and 8 present isothermal scans of the real and imaginary part of electric modulus as a function of frequency, for the composites with 3%, and 10%w/w content in $BaTiO_3$ particles, at temperatures varying from 30 to 150°C. Concerning the $M' = F$ (log (f)) diagrams, the existence of a clear "step-like" transition from low to high values of (M'), at moderate frequencies, is evident. The recorded transition shifts to higher frequencies with increasing temperature and $BaTiO_3$ content. In the $M'' = F$ (log (f)) plots and in the vicinity of this transition dielectric loss peaks are clearly formed. The temperature–frequency superposition shifts peaks towards higher frequencies as temperature is raised, since at elevated temperatures dipoles acquire enhanced thermal energy being thus able to follow faster alternations of the applied field. As a consequence relaxation time of the occurring process becomes shorter. The recorded relaxation process, present also in the pure novolac spectra, is attributed to the glass to rubber transition of the polymer matrix (α-relaxation), where large parts of the polymer chain relax simultaneously.[26]

Figure 9 presents comparative isochronal plots, for all the tested samples, of loss modulus index as a function of temperature at two different frequencies. In Figure 9(a) (f = 1 Hz) a wide loss peak is present in the low temperature range, which is assigned to α-mode, and is the same process with the one recorded in Figures 7 and 8. It should be noted that

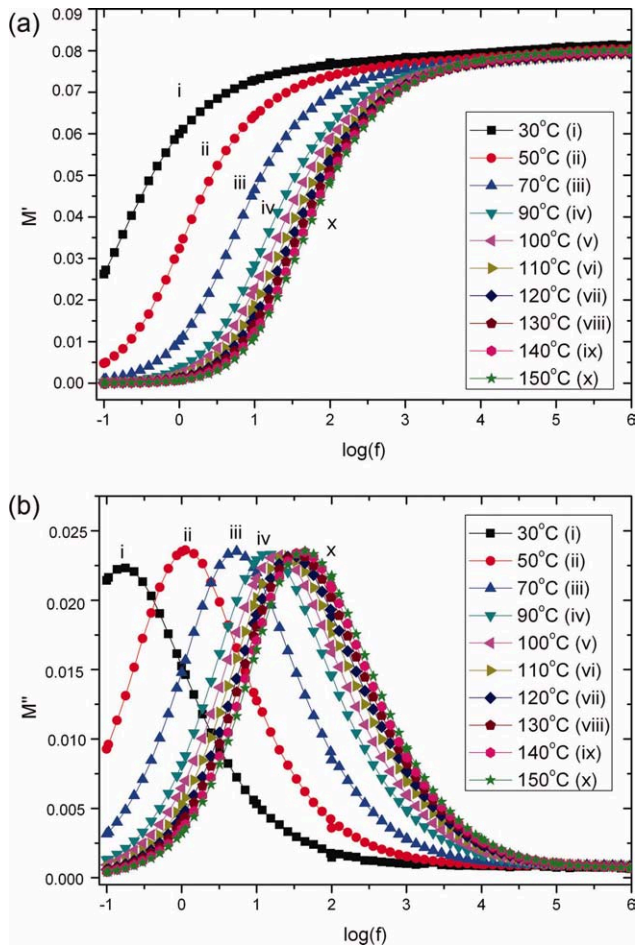

Figure 8 Real (a) and imaginary (b) part of electric modulus versus frequency for the specimen with 10% w/w content in $BaTiO_3$, at various temperatures. [Color figure can be viewed in the online issue, which is available at wileyonlinelibrary.com.]

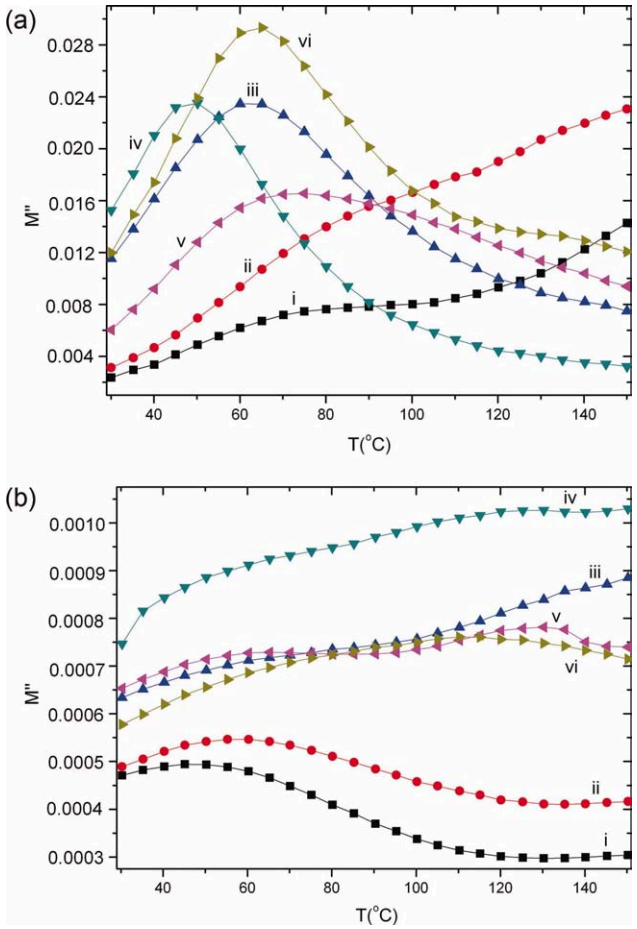

Figure 9 Loss modulus index as a function of temperature at (a) $f = 10^{\circ}$ Hz and (b) $f = 10^5$ Hz for all the examined specimens. Specimens' notation is the same with the one in Figure 4. [Color figure can be viewed in the online issue, which is available at wileyonlinelibrary.com.]

for the systems with $BaTiO_3$ content varying from 0 to 10% w/w loss peak position shifts to lower temperatures systematically indicating lowering of glass transition temperature with ceramic filler content. This type of behavior has been attributed to weak interactions between filler and polymer matrix or to moderate adhesion level of the nanoinclusions by the matrix.[27,28] In the high temperature range of Figure 9(a) a hump can be observed in the dielectric spectra, implying the existence of another process. This process is slower than α-mode, characterized by larger relaxation time, and is easier detectable in the spectra of nanocomposites. The physical origin of the process is attributed to interfacial polarization, resulting from the accumulation of unbounded charges at the interface of the systems. Charges arise from the stage of specimens' preparation, and at the interface between filler and matrix form large dipoles, which fail to align themselves parallel to the applied field with increasing frequency, giving thus a relaxation process.[22–24] Interfacial polarization is present in electrically heterogeneous systems, but

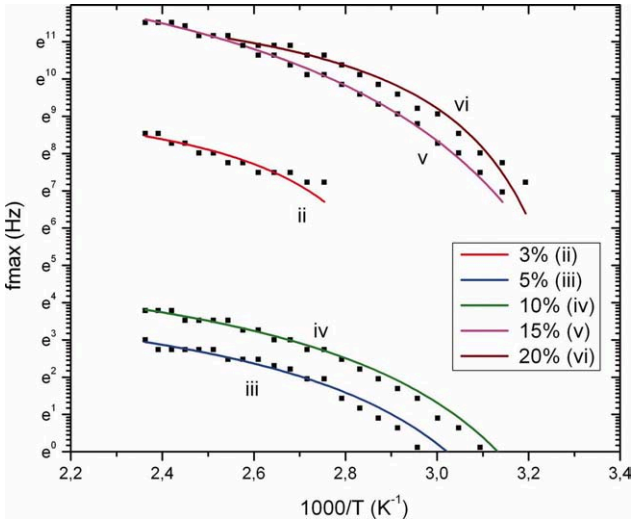

Figure 10 Loss peak position as a function of the reciprocal temperature for α-relaxation process, for all the nanocomposite systems. The indicated percentages correspond to the w/w content in $BaTiO_3$. [Color figure can be viewed in the online issue, which is available at wileyonlinelibrary.com.]

also in polymers because of the presence of additives, plasticizers, impurities, etc.[22–24] Figure 9(b) displays the electric modulus loss spectra as a function of temperature, at $f = 10^5$ Hz. The aforementioned processes shift to higher temperatures, and a new one in the low temperature region inserts in the experimental "window". Since it is recorded at low temperatures and high frequency is the faster relaxation mechanism present in all systems including pure novolac. This process (β-mode), which is relatively weaker, is ascribed to reorientation of polar side groups of the main chain of the matrix. Novolac resin contains such polar groups (i.e., –OH and/or –CH_3).[25]

The dielectric response of the samples with 15% w/w and 20% w/w in $BaTiO_3$ content deviates significantly from the corresponding ones of the other composites due to their high porosity and possible air trapping in their bulk body. Thus these results, although shown in this study, are not considered as reliable and thus are not further analyzed.

The temperature dependence of the loss peak position for the main dielectric relaxation process is

TABLE III
Fitting Parameters of VFT Equation for 3% w/w, 5% w/w, 10% w/w, 15% w/w, 20% w/w in BaTiO3 Examined Systems

Sample	T_0 (K)	A
Resin + 3% w/w $BaTiO_3$	321.0	0.39
Resin + 5% w/w $BaTiO_3$	283.7	0.74
Resin + 10% w/w $BaTiO_3$	275.0	0.87
Resin + 15% w/w $BaTiO_3$	265.1	1.47
Resin + 20% w/w $BaTiO_3$	290.0	0.48

depicted in the Arrhenius plot of Figure 10. As it can be seen data of loss peak frequency versus reciprocal temperature, for all nanocomposites, remarkably deviate from a pure Arrhenius-type behavior. Data can be fitted via the Vogel-Fulcher-Tamann (VFT) equation, which accounts that relaxation rate increases rapidly at lower temperatures because of the reduction of free volume. VFT is expressed by eq. (2):

$$f_{\max} = f_0 \exp\left(-\frac{AT_0}{T - T_0}\right) \quad (2)$$

where f_0 is a pre-exponential factor, A is a constant being a measure of the activation energy of the process, T_0 the Vogel temperature or ideal glass transition temperature, and T the absolute temperature. Fitting parameters of eq. (2) for the nanocomposite systems are listed in Table III. The agreement between data and produced curves provides an additional indication for the physical origin of the recorded process in Figures 7 and 8, since it is widely accepted that glass to rubber relaxation mechanism (α-mode) exhibits a VFT behavior.[26–28] Further, it should be noted that T_0 diminishes with barium titanate content following the same qualitative tendency with that of glass transition temperature as derived from Figure 9(a).

CONCLUSIONS

Polymer nanocomposites consisting of novolac resin and barium titanate nanoparticles were prepared and studied. Mechanical and dielectric behavior was investigated experimentally by means of shear and bending tests and broadband dielectric spectroscopy respectively. Mechanical performance becomes worse with the presence of ceramic filler, indicating poor adhesion between matrix and nanoparticles. All samples exhibit brittle fracture with no evidence of necking. On the contrary barium titanate nanoparticles improve the dielectric response of the composite systems by raising the values of permittivity in the whole frequency range. Especially at the low frequency edge the reinforcing efficiency of ceramic particles enhances permittivity by a factor close to 2 at ambient, with respect to the pure novolac, which exceeds 8 at 150°C. The variation of real part of dielectric permittivity with barium titanate content and temperature indicates that this type of composites can be proved useful in developing of energy storing devices. Concerning the dielectric relaxations, three distinct mechanisms have been detected. From the slower to the faster one, they have been attributed to interfacial polarization, glass to rubber transition of the polymer matrix (α-mode) and reorientation of polar side groups of the polymer chain (β-mode). Dielectric relaxations data imply reduce of glass transition temperature with barium titanate content, which could be related to weak interaction between the constituents and/or insufficient adhesion of the ceramic particles by the polymer matrix.

References

1. Psarras, G. C. Express Polym Lett 2008, 2, 460.
2. Parthenios, J.; Psarras, G. C.; Galiotis, C. Compos Part A-Apll S 2001, 32, 1735.
3. Popielarz, R.; Chiang, C. K.; Nozaki, R.; Obrzut, J. Macromolecules 2001, 34, 5910.
4. Korotkov, N.; Gridnev, S. A.; Konstantinov, S. A.; Klimentova, T. I.; Barmin, Y. V.; Babkina, I. V. Ferroelectrics 2004, 299, 171.
5. Jylhä, L.; Honkamo, J.; Jantunen, H.; Sihvola, A. J Appl Phys 2005, 97, 104104.
6. Patsidis, A.; Psarras, G. C.,Express Polym Lett 2008, 2, 718.
7. Dang, Z.-M.; Shen, Y.; Nan, C.-W. Appl Phys Lett 2002, 81, 4814.
8. Dang, Z.-M.; Lin, Y.-H.; Nan, C.-W. Adv Mater 2003, 15, 1625.
9. Ramajo, L.; Reboredo, M.; Castro, M. Compos Part A-Apll S 2005, 36, 1267.
10. Hamami, H.; Arous, M.; Lagache, M.; Kallel, A. Compos Part A-Apll S 2006, 37, 1.
11. Choudhury, A. Mater Chem Phys 2010, 121, 280.
12. Dang, Z.-M.; Yu, Y.-F.; Xu, H.-P.; Bai, J. Compos Sci Technol 2008, 68, 171.
13. Thomas, P.; Satapathy, S.; Dwarakanath, K.; Varma, K. B. R. Express Polym Lett 2010, 4, 632.
14. Ramajo, L.; Reboredo, M. M.; Castro, M. C. Int J Appl Ceram Tec 2010, 7, 444.
15. Ioannou, G.; PatsidisA.; Psarras, G. C. Compos Part A-Apll S 2011, 42, 104.
16. Simitzis, J. Angew Makromol Chem 1989, 165, 21.
17. Braun, D.; Cherdron, H.; Kern, W. Praktikum der makromolekularen organischen Chemie, Dr. Alfred Huthig Verlag Heidelberg,1971.
18. Simitzis, J.; Karagianis, K.; Zoumpoulakis, L. Eur Polym J 1996, 32, 857.
19. Simitzis, J.; Karagianis, K.; Zoumpoulakis, L. Polym Int 1995, 38, 183.
20. Orthamann, Mair: Die Prufung thermoplastischer Kunstoffe 1971, p55.
21. BÜrger, A. Kohlenstoffasen-Verstārker Polymere und deren Ehernischer, Abbaw bis zu Khlenstoff/Kohlenstoff-Verbundwerkstoffen, Dissertation1973.
22. Tsangaris, G. M.; Psarras, G. C.; Kouloumbi, N. J Mater Sci 1998, 33, 2027.
23. Psarras, G. C.; Manolakaki, E.; Tsangaris, G. M. Compos Part A-Apll S 2003, 34, 1187.
24. Kontos, G. A.; Soulintzis, A. L.; Karahaliou, P. K.; Psarras, G. C.; Georga S. N.; Krontiras, C. A.; Pisanias M. N. Express Polym Lett 2007, 1, 781.
25. Simitzis, J.; Zoumpoulakis, L.; Soulis, S.; Triantou, D.; Pinaka, C. J Appl Polym Sci 2011, 121, 1890.
26. Kremer, F.; Schönhals, A. In Broadband Dielectric Spectroscopy; Kremer, F.; Schönhals, A., Eds.; Springer: Heidelberg, 2003;, Chap. 4.
27. Psarras, G. C. In Physical Properties and Applications of Polymer Nanocomposites; Tjong, S. C.; Mai, Y.-W., Ed.; Woodhead Publishing Limited: Oxford, 2010; Chap. 2.
28. Kalini, A.; Gatos, K. G.; Karahaliou, P. K.; Georga, S. N.; Krontiras, C. A.; Psarras, G. C. J Polym Sci B Pol Phys 2010, 48, 2346.